Spiral-like continuous spin-reorientation transition of Fe/Ni bilayers on Cu(100)

R. Ramchal,[1] A. K. Schmid,[2] M. Farle,[1] and H. Poppa[2]
[1]*Institut für Physik, Universität Duisburg-Essen, Lotharstrasse 1, 47048 Duisburg, Germany*
[2]*NCEM, Lawrence Berkeley National Laboratory, Berkeley, California 94720, USA*
(Received 4 December 2003; revised manuscript received 4 March 2004; published 2 June 2004)

The magnetic domain microstructure of 0 to 3 monolayers (ML) of Fe on 7.2 and 11 ML Ni/Cu(100) films was studied by spin-polarized low-energy electron microscopy at 300 K. The 11 ML Ni layers showed perpendicular oriented stripe domains of some micrometers in width parallel to the atomic step edges of the Cu(100) substrate, whereas the magnetization of the 7.2 ML Ni film was in a canted state. For both Ni layers, perpendicular oriented domains are stabilized upon Fe deposition up to 2.5 ML Fe without changing the original Ni domain pattern significantly. Between 2.5 and 2.9 ML the domains break up into smaller stripe domains, and the magnetization of the coupled Fe/Ni bilayer continuously rotates within the oppositely oriented magnetic stripe domains into the film plane by an in-plane 74° spiral-like motion. At 2.9 ML Fe large (10 μm) in-plane magnetic domains appear. From the critical Fe thickness of 2.7 ± 0.2 ML we find that the Fe/Ni interface magnetic anisotropy is $K^{S}_{2,\text{Ni-Fe}} = -93$ μeV/atom favoring an in-plane easy axis.

DOI: 10.1103/PhysRevB.69.214401 PACS number(s): 75.70.Ak, 34.80.Nz, 75.70.Kw, 75.30.Kz

In the last decades much attention has been paid to the thickness and temperature driven spin reorientation of ultrathin films. Two prototypical systems that have been studied intensively are Fe/Cu(100) (Refs. 1–6) and Ni/Cu(001) (Refs. 7–11). Due to the spin-orbit induced surface anisotropy, which favors perpendicular magnetization in Fe/Cu(100), a spin-reorientation transition (SRT) from out-of-plane to in-plane takes place with increasing film thickness and temperature. Ni/Cu(100) on the other hand has a reversed SRT from in-plane to out-of-plane, due to its surface anisotropy favoring in-plane magnetization and a large volume anisotropy favoring out-of-plane magnetization which arises from the face-centered-tetragonal (fct) distorted crystal structure of Ni on Cu.[8] The combination of both Fe and Ni makes the coupled system an interesting case to study the relation between the structure, magnetism, and coupling phenomena of Fe/Ni bilayers on Cu(100). Some investigations of this system have been performed previously. Using magneto-optic Kerr effect the magnetic interlayer exchange coupling as a function of different Fe and Ni layer thicknesses was studied as a function of temperature[12] and the pronounced influence of the Fe/Ni interface on the SRT was observed.[13] An exchange bias due to two superstructure phases within the Fe film was also found.[14] Earlier measurements by low-energy electron diffraction and x-ray magnetic circular dichroism (XMCD) revealed the correlation between structural and magnetic phases and the existence of an antiferromagnetic state in the Fe interior within the fcc phase[15] similar to results for Fe/Cu(100).[16] Recent experiments using photoemission electron microscopy have been performed on Cu capped Ni/Fe/Co/Cu(100) thin-film systems to study the interlayer coupling within the trilayer.[17] To the best of our knowledge, however, no investigation on the micromagnetic domain structure of uncapped Fe/Ni bilayers on Cu(100) using domain imaging methods has been done so far.

In the present work, spin-polarized low-energy electron miroscopy (SPLEEM) is used to analyze the magnetic domain structure of the bilayer Fe/Ni as a function of the Fe layer thickness near the SRT, which occurs around 2.5 ML Fe at room temperature. SPLEEM is a surface sensitive method with a lateral resolution of 10 nm and an image acquisition rate of about eight frames per second. SPLEEM images were recorded before, during and after *in situ* film growth. Exploiting the method's sensitivity to topographic features such as atomic surface steps and step bunches and its capability to simultaneously record magnetic contrast images, we were able to directly correlate topography and magnetic domain formation during deposition.

A 10 mm diameter Cu(100) single-crystal substrate with a miscut angle below 0.1° was used for all experiments. In order to suppress the formation of atomic step bunches at the copper surface we used a carefully developed substrate cleaning procedure.[18] During 12 h of Ar-ion sputtering using a low current of 0.1 μA/cm^2 and an ion energy in the range of 1.5–3 kV the Cu substrate was automatically flash annealed to $\approx$1000 K in 10 min intervals. After this preparation schedule, no surface contamination was detectable using a single-pass cylindrical mirror Auger electron spectrometer. LEEM (Ref. 19) images of the cleaned Cu(100) crystal confirmed that the surface had atomically flat terraces separated mostly by monoatomic steps.

Fe/Ni films were deposited *in situ* from separate *e*-beam evaporators onto the Cu(100) substrate at 300 K. The base pressure during imaging was 2×10^{-8} Pa, the maximum pressure during evaporation was 4×10^{-8} Pa. The Ni grows pseudomorphic with the Cu lattice constant in-plane up to about 10 monolayers (ML) thickness in a tetragonally distorted (fct) crystal structure.[20] The Fe layers of up to 3 ML thickness are expected to adapt this fct structure. The formation of 1 ML of a FeNi alloy at the interface cannot be excluded at room-temperature deposition.

The same setup was used for magnetic domain imaging by SPLEEM. A spin-polarized, low-energy electron beam is directed towards the sample surface at normal incidence, and the specular beam of the resulting, backscattered electron-diffraction pattern is magnified in an electron-optical column to form a real-space image of the sample surface. By monitoring the average intensity of the image beam the SPLEEM

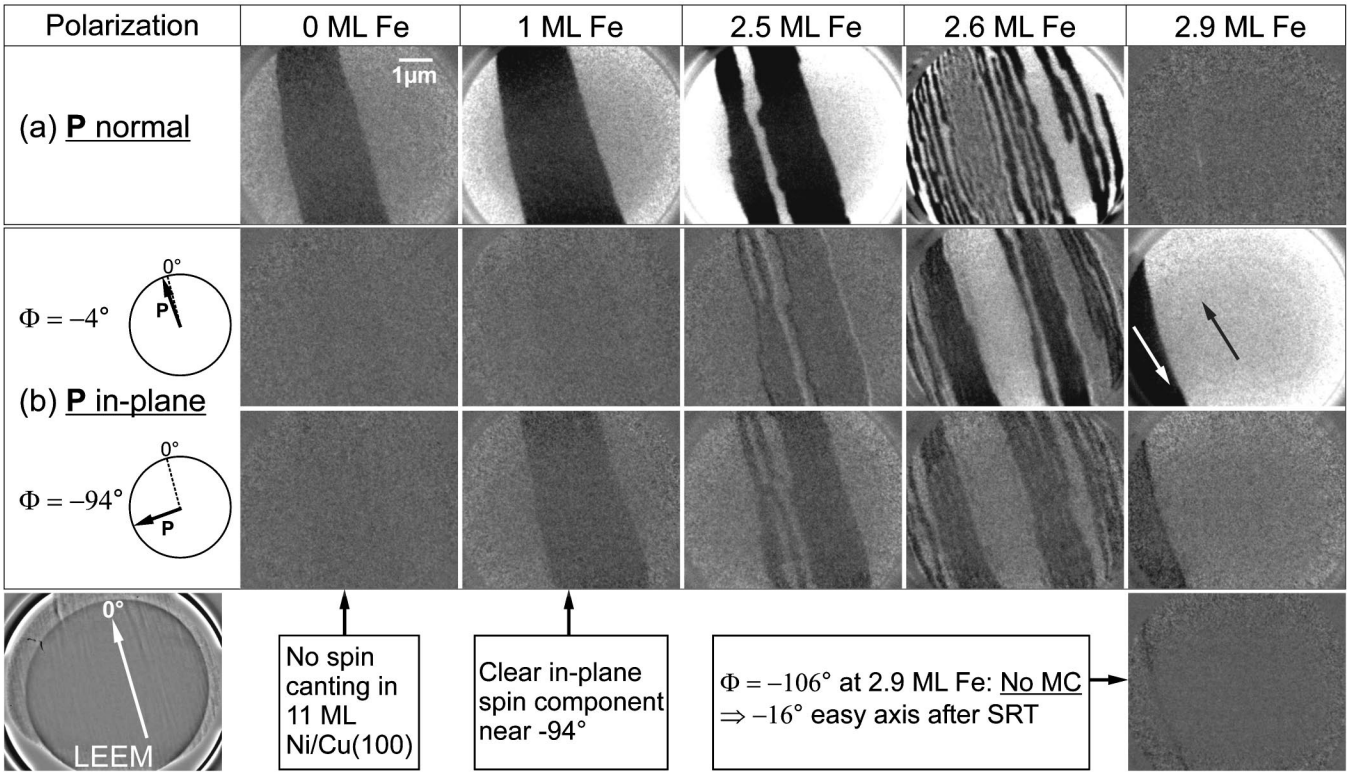

FIG. 1. Spin-reorientation transition of a *x* ML Fe/11 ML Ni bilayer on Cu(100) at 300 K as a function of the Fe layer thickness. The SRT takes place by a continuous spin rotation, a break up of domains into stripe domains and a reformation to large in-plane domains at 2.9 ML Fe, where the out-of-plane magnetic contrast (MC) has vanished (a). For details see text.

can be used for convenient and very precise film thickness control during *in situ* film growth as described in Ref. 2. The periodic nucleation, growth, and completion of atomic monolayers during epitaxial growth leads to well-known diffraction intensity oscillations.[21] The distance between two maxima corresponds to one atomic layer giving the deposition rate, i.e., typically 0.2 ML and 0.1 ML per min for the Ni and the Fe evaporator, respectively.

Before discussing our results on the magnetism of Fe/Ni/Cu(100), we briefly describe how magnetic contrast (MC) originates within this microscope. The magnetic contrast in SPLEEM images is related to the relative orientations of the magnetization **M** in the film and the beam polarization **P** according to $\mathrm{MC} \propto \mathbf{P} \cdot \mathbf{M}$. Being based upon spin-dependent exchange scattering of the spin-polarized illuminating beam, the magnetic image contrast between the reflected intensities for electrons having their polarizations parallel and antiparallel with respect to the local sample magnetization is typically of the order of 1%. To enhance the contrast, we toggled the illumination polarization by 180° from image to image, so that a differential imaging method can be employed.[22] The method is based on the usual definition of the exchange asymmetry $A_{\mathrm{ex}} = 1/|\mathbf{P}|(I_+ - I_-)/(I_+ + I_-)$ where I_+ and I_- represent the reflected intensities for oppositely polarized incident beams. Subtraction of I_+ (spin-up) and I_- (spin-down) images in the numerator eliminates nonmagnetic diffraction and topographical image features. Only features, which originate exclusively from the magnetism of the sample are left in the image.

In the instrument used here, the electron beam passes through a spin-manipulator prior to illuminating the sample. The spin manipulator allows for a rotation of the beam polarization in both the polar and the azimuthal angular orientation. Imaging with various beam polarizations allows a complete characterization of the local magnetization vector in the sample surface. For details concerning the instrument see Ref. 18, and references therein. Since the exchange asymmetry oscillates with energy due to the spin-dependent band structure[23] the optimum energy for a maximum magnetic contrast has to be chosen for Fe and Ni individually. Following the procedure described in Ref. 18 we found an electron energy of $E = 9.5$ eV for optimum magnetic contrast of Ni domains and $E = 4.5$ eV for imaging Fe domains.

Two different Ni underlayer thicknesses were chosen for the magnetization reorientation studies of Fe/Ni/Cu(100) bilayers, a 7.2 ML Ni film in a slightly out-of-plane canted state and an 11 ML Ni film with fully perpendicular anisotropy, which were characterized before Fe deposition.

For the following discussion of magnetization and spin-polarization directions, we use spherical coordinates with the azimuthal angle Φ measured in the counterclockwise direction and $\Phi = 0°$ corresponding to the direction of step edges of the Cu(100) substrate, as sketched on the left in Fig. 1(b). The perpendicular orientation of the magnetization within the 11 ML Ni/Cu(100) film was confirmed by imaging the magnetic domain structure of the film in perpendicular and several in-plane orientations of the electron-beam polarization **P** as shown in Fig. 1 (''0 ML Fe''). The magnetic do-

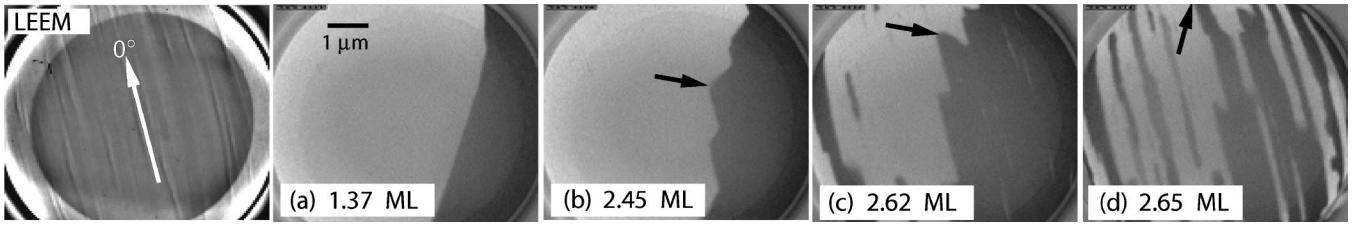

FIG. 2. Domain images for the vertical component of the magnetization as a function of Fe thickness on 7.2 ML Ni/Cu(100) at 300 K (a)–(d). Stripe domains evolve out of the original domain wall. The stripe domains are parallel to the Cu atomic step edges (0°) seen in the LEEM image of the bare Cu substrate above. The domain wall width increases slightly from 130 ± 5 nm at the start of the SRT to an average width of 150 ± 5 nm at the maximum number of stripes.

main pattern of the Ni film consists of stripes of several micrometers width with a perpendicularly up or down oriented magnetization (z direction) (a). No in-plane magnetization components were found in this pure Ni film. For example, the two images in the leftmost column (0 ML Fe) in Fig. 1(b) were acquired with spin polarizations oriented along two orthogonal in-plane directions at $\Phi=-4°$ and $-94°$. The absence of MC in these images confirms that there is no spin canting in the Ni/Cu(100) film of 11 ML (b). Upon Fe deposition on top of the Ni/Cu(100) film the change of the domain pattern and the magnetization direction is demonstrated in the sequence of images shown in Fig. 1. The deposition of 1 ML Fe results in an increase of the magnetic contrast along the perpendicular direction and a slight broadening of the Ni domain pattern as well as a narrowing of the average domain wall width from ~280 nm to ~190 nm. Upon further Fe deposition the out-of-plane MC [Fig. 1(a)] increases up to 2.5 ML Fe, at which the onset of the formation of narrower domains is observed which corresponds to the start of the SRT. As the Fe layer thickness is further increased, the large out-of-plane domains break up into ~250 nm wide stripe domains. The correlation of the shape of the magnetic domains with the topography of the Cu crystal is revealed by the LEEM image of the bare Cu surface shown in Fig. 1. The domain walls of the stripe domains are aligned parallel to the Cu atomic steps. Finally, the MC in perpendicular orientation vanishes at 2.9 ML Fe proving that the magnetization is completely in the film plane. In order to determine the easy axis of the in-plane magnetized domains at 2.9 ML Fe, the electron-beam polarization **P** was rotated till the MC between the domains vanished. Since the MC vanishes at $\Phi=-106°$, the magnetization orientation within the domains lies perpendicular to this angle, i.e., the magnetization within the domains is parallel and antiparallel at an angle $\Phi=-16°$ with respect to the step edges. No magnetization orientation at 90° with respect to this direction was found as might be expected for a cubic system. The contrast at $\Phi=-106°$ vanishes and reveals a broad (≈300 nm) Néel wall by the line of darker contrast on the left side of the image. Within the wall the spins rotate in the film plane.[18] A Bloch wall would not cause any magnetic contrast in the middle of the wall for the given **P**.

Since we had no technique available to verify the crystal orientation in our setup, we can only make the following reasonable assumption about the relation of the domain pattern to the crystallographic direction. It is known that Ni/Cu(100) favors the [011] in-plane direction in the thickness range above 6 ML,[7] while Fe/Cu(100) favors a [001] in-plane orientation with a much larger in-plane anisotropy than for Ni/Cu(100). Therefore, in the coupled Fe/Ni/Cu(100) system the [001] direction most likely is the easy axis. As shown above, the $-16°$ direction is the easy axis of the 2.9 ML Fe/Ni magnetization, which we interpret to be parallel to the [001] crystallographic axis of the bilayer. Based on these reasonable assumptions regarding the orientation of our crystal, the step edges as seen in the LEEM image (Fig. 2 left) do not run along a low-index crystallographic direction like the ⟨011⟩ which is known to be a low-energy step direction on Cu surfaces vicinal to [100].[24,25]

The break up of the domains is also observed for the two in-plane directions [Fig. 1(b)] unambiguously showing that the magnetization of the bilayer is canted within the stripes. The canting angle with respect to the film normal increases with Fe coverage as seen by the increase of the MC in the top in-plane image series of Fig. 1(b). The reorientation of the magnetization from perpendicular to in-plane with increasing Fe layer thickness occurs via a break up of the original domain pattern and a simultaneous continuous rotation of **M** within the individual domains. One may notice that the in-plane components $\mathbf{M}_{\parallel}^{+}$, $\mathbf{M}_{\parallel}^{-}$ of the canted oppositely ori-

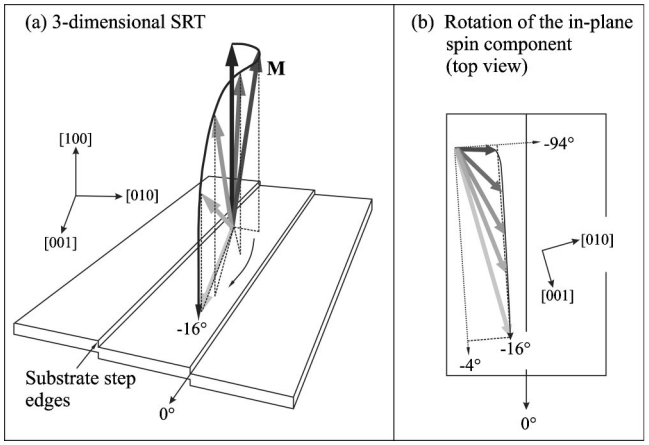

FIG. 3. (a) Spiral-like spin reorientation of x ML Fe/11 ML Ni/Cu(100) films from perpendicular to in-plane orientation with increasing Fe layer thickness ($x=0...3$ ML). The in-plane spin component rotates from $-90°$ to $-16°$, i.e., [001] direction, by an angle of 74° within the plane. (b) In agreement with the SPLEEM data the projection onto the $-94°$ direction remains almost constant.

ented domains would not be detectable by a technique such as second-harmonic generation[11] or x-ray magnetic circular dichroism[25] which averages over large areas.

Interestingly, at a coverage of 1 ML Fe magnetic contrast abruptly appears also for the polarization vector **P** at $\Phi = -94°$ [Fig. 1(b) in-plane bottom series of images]. There is nearly no MC for 1 ML Fe, if **P** is set at $\Phi = -4°$, which is perpendicular to the image above. At higher Fe coverages the contrast becomes much stronger for **P** along $\Phi = -4°$ and stays constant for **P** along $\Phi = -94°$. The refined analysis reveals that the in-plane easy axis of the magnetization $\mathbf{M}_{\|}$ is given by $\Phi = -90°$ for 1 ML Fe on 11 ML Ni and by $\Phi = -16°$ (along [001]) for 2.9 ML Fe. The in-plane component of the magnetization rotates from $-90°$ before to $-16°$ (the [001] direction) after the SRT. These in-plane orientations were observed for both Ni thicknesses. The unusual direction of the in-plane component of **M** at $-90°$ could be explained by the interplay of the magnetic anisotropy induced by the step edges which favors the direction parallel $\langle 011 \rangle$ to the step edges for strained Ni films and the bulk magnetoelastic contribution which favors an easy axis perpendicular to the surface and, thus, also to some degree perpendicular to the step edges. At larger Fe thickness the in-plane anisotropy of Fe dominates favoring the $\langle 001 \rangle$ direction. The sketch in Fig. 3 illustrates the spiral-like reorientation which is the complex superposition of the spin reorientation from out-of-plane to in-plane and the simultaneous rotation of the in-plane component from $-90°$ to $-16°$. Interestingly, the MC in the $-94°$ orientation of Fig. 1(b) stays nearly constant throughout the SRT. In the suggested reorientation procedure of Fig. 3 the arrowheads of the in-plane spin vectors lie on a slight curve, so that the projection of the in-plane spin component onto the $-94°$ direction remains almost constant. This nicely explains the unchanged magnetic contrast in the $-94°$ direction shown in Fig. 1(b).

The same reorientation behavior was found for bilayers with a 7.2 ML Ni underlayer which was in a canted spin state with the in-plane component of the spins pointing into the $-94°$ direction. Again there was no magnetic contrast detected in the $-4°$ polarization orientation for Fe coverages below 1 ML but in $-94°$ orientation. The MC remained nearly constant for the $\Phi = -94°$ direction, whereas the MC in $-4°$ increased only weakly up to a Fe coverage of 2.5 ML followed by a dramatically increase just at the thickness where the domains break up into stripes. The direction of the magnetization within the in-plane domains after the SRT again was along [001] ($-16°$), confirming the same spiral-like reorientation as found for the bilayer with 11 ML Ni.

The onset of the formation of the stripe domains is discussed in greater detail in the following. A domain wall of the bilayer with 7.2 ML Ni was imaged as a function of Fe deposition (Fig. 2). No correlation of the direction of that wall segments with topographic features was found by comparing the magnetic SPLEEM images with the LEEM image of the Cu crystal surface. Starting at about 1.4 ML Fe, where a linear domain wall was observed (a), the domain wall started to adjust to the substrate step edges by forming rectangular protrusions with one side running parallel to the direction of the Cu atomic steps [(b) and (c)]. This process evolves into a stripe domain pattern along the step direction (d). At about 2.6 ML Fe (c) stripe domains also appear spontaneously within the domains. The average stripe domain width at the maximum number of stripes (not shown here) is about 280 nm.

Below 10 eV electron energy, the penetration depth of the spin-polarized beam can be as large as several 10 Å, and the whole bilayer contributes to the formation of contrast. In order to check if the magnetization of the Ni and the Fe layers remain parallel to each other during the SRT, element-specific hysteresis loops were recorded by XMCD. They show that the Ni and the Fe layers are coupled ferromagnetically and stay parallel throughout the SRT.

To describe the nature of a continuous magnetization reorientation transition the magnetic anisotropy constants of second and fourth order have to be considered.[7] The orientation of the magnetization in ultrathin films is determined by the balance between the intrinsic magnetic anisotropy energy (MAE), which arises from spin-orbit coupling and the shape anisotropy which is of dipolar origin. The shape anisotropy always favors an in-plane easy axis for thin films, the intrinsic MAE may either favor in-plane or perpendicular orientation. The balance between the two anisotropy contributions varies as a function of film thickness and temperature. A SRT from a perpendicular to an in-plane easy axis will occur when the shape anisotropy dominates over the intrinsic anisotropy. The easy axis of magnetization is determined by the minimum of the free-energy density E per unit area which in the case of the tetragonal bilayer system Fe/Ni on Cu(100) includes the following contributions:

$$
\begin{aligned}
E = & \left(\frac{1}{2}\mu_0 M_{\mathrm{Ni}}^2 - K_{2,\mathrm{Ni}}^{V} \right) \cos^2\theta \, d_{\mathrm{Ni}} \\
& + \left(\frac{1}{2}\mu_0 M_{\mathrm{Fe}}^2 - K_{2,\mathrm{Fe}}^{\mathrm{V}} \right) \cos^2\theta \, d_{\mathrm{Fe}} - K_2^{\mathrm{S,eff}} \cos^2\theta \\
& - \frac{1}{2} K_{4\perp}^{\mathrm{eff}} \cos^4\theta - \frac{1}{8} K_{4\|}^{\mathrm{eff}} (3 + \cos 4\Phi) \\
& \times \sin^4\theta - J \mathbf{M}_{\mathrm{Ni}} \cdot \mathbf{M}_{\mathrm{Fe}}, \\
& \text{where} \quad K_2^{\mathrm{S,eff}} = K_{2,\mathrm{Ni\text{-}Cu}}^{\mathrm{S}} + K_{2,\mathrm{Ni\text{-}Fe}}^{\mathrm{S}} + K_{2,\mathrm{Fe\text{-}vac}}^{\mathrm{S}} \qquad (1)
\end{aligned}
$$

and

$$
\begin{aligned}
K_i^{\mathrm{eff}} = & K_{\mathrm{i,Ni}}^{\mathrm{V}} d_{\mathrm{Ni}} + K_{\mathrm{i,Fe}}^{\mathrm{V}} d_{\mathrm{Fe}} + K_{\mathrm{i,Ni\text{-}Cu}}^{\mathrm{S}} + K_{\mathrm{i,Ni\text{-}Fe}}^{\mathrm{S}} \\
& + K_{\mathrm{i,Fe\text{-}vac}}^{\mathrm{S}} \quad \text{with} \quad i = 4\perp, 4\|.
\end{aligned}
$$

θ is the polar angle of the magnetization with respect to the [100] direction, Φ is the azimuthal angle measured against the easy [001] in-plane direction of the system. J is the ferromagnetic coupling constant between the magnetizations M_{Ni} and M_{Fe} of Ni and Fe, which are always aligned parallel as shown by our XMCD measurements. K_2, $K_{4\perp}$, and $K_{4\|}$ are the second- and the fourth-order perpendicular and in-plane terms of MAE. K^{V} denotes the volume contribution and K^{S} the various surface and interface anisotropies as given by the lower index. For $K_{4\perp} = K_{4\|} = 0$ no tilted orien-

TABLE I. Anisotropy constants at 300 K.

		Reference
$K^{V}_{2,Ni}$	30 μeV/atom	7
$K^{V}_{2,Fe}$	77.7 μeV/atom	27
$K^{S}_{2,Ni\text{-}Cu}$	-59 μeV/atom	26
$K^{S}_{2,Fe\text{-}vac}$	64 μeV/atom	5 and 27

tation of the magnetization is possible, and hence if K_2 changes, a *discontinuous* flip of the magnetization is expected.[7] Due to the fact that we unambiguously find an out-of-plane spin canting as well as a continuous rotation of the magnetization, the second-order contributions to the MAE alone are not sufficient to account for this behavior. This means that in the theoretically strict sense a fourth-order contribution would have to be included in the analysis. However, the reorientation interval of 0.4 ML Fe is very small, i.e., the K_4 values are small, and we neglect them in the further analysis. Only for $K_4 \gg K_2$ the difference between the critical thicknesses d_{c1} and d_{c2} for the onset and end of the SRT becomes significant.[7] It should be noted that SPLEEM is a good technique to reveal even this very small difference between the lower and the upper critical thickness which makes it easier to determine the nature of a transition. In other words we consider the 0.4 ML interval as a discontinuous flip of M_{tot} at the mean value $d_{c,Fe}=2.7$ ML in the following approximation.

In this simplified model, the sum of the shape anisotropy and the crystalline anisotropy contributions vanishes at $d_{c,Fe}$:

$$\left(\frac{1}{2}\mu_0 M^2_{Ni} - K^{V}_{2,Ni}\right) d_{Ni} + \left(\frac{1}{2}\mu_0 M^2_{Fe} - K^{V}_{2,Fe}\right) d_{c,Fe} - K^{S}_{2,Ni\text{-}Cu} - K^{S}_{2,Ni\text{-}Fe} - K^{S}_{2,Fe\text{-}vac} = 0. \quad (2)$$

In the discussion which of the various contributions plays the major role for the observed SRT, one can consider two scenarios. In the first case, one can assume that a sharp interface between the Fe and Ni layers exists. In this case the volume, interface, and surface contributions for Fe and Ni monolayers on Cu can be taken from the literature (Table I). The shape anisotropy of the bilayer structure increases from 7.5 μeV/atom (Ref. 9) to 32 μeV/atom (averaged for the bilayer) by the deposition of Fe due to the 3.5 times larger magnetic moment of the Fe atoms ($2.22\mu_B$) compared to the Ni atoms ($0.62\mu_B$) in bulk. Using these values together with the literature values of the anisotropies listed in Table I, one realizes that the sum of these quantities is zero only, if a large negative interface anisotropy $K^{S}_{2,Ni\text{-}Fe}=-93$ μeV/atom is present. Thus, this large interface anisotropy is needed to explain the critical thickness of 2.7 $\pm$0.2 ML for the SRT. Note that for Fe/Cu(001) where no Ni-Fe interface is present the magnetization of 3 ML Fe grown at room temperature is oriented perpendicular to the surface.[2] In a second more realistic approach one can consider the existence of an intermixed interface consisting of an 50:50 FeNi alloy over 2 ML. According to the Slater-Pauling curve the average magnetic moment per atom in these two layers is $1.7\mu_B$. Recalculation of the shape anisotropy of the Fe/Ni bilayer with a 2 ML thick alloyed interface region while keeping the deposited number of Fe and Ni atoms constant yields an increase of the shape anisotropy by about 8% only. Hence, we can conclude that the increase of the shape anisotropy as a function of Fe deposition is not sufficient to force the magnetization of the bilayer into the film plane. A relatively large Fe-Ni interface anisotropy needs to be taken into account to explain the critical Fe thickness at which the SRT occurs.

In summary, the domain structure of Fe/Ni bilayers on Cu(100) for 0 to 3 ML Fe on 7.2 ML and 11 ML Ni was studied by spin-polarized low-energy electron microscopy at 300 K. The 11 ML Ni film showed perpendicularly magnetized stripe domains of 1–2 μm width, whereas the 7.2 ML Ni film was in a canted magnetization state. The spin-reorientation transition from out-of-plane to in-plane as a function of the Fe layer thickness occurs via the formation of a multidomain state and the simultaneous continuous rotation of the magnetization vector within the domains. The 250 nm wide stripe domains are oriented parallel to the Cu atomic step edges within a Fe thickness interval of 0.4 ML on both Ni underlayers. No significant difference in the reorientation process between the Fe films grown on 7.2 ML canted and 11 ML perpendicularly magnetized Ni film was found. The driving forces for the SRT from perpendicular to in-plane were identified as the increased shape anisotropy due to the large magnetic moment of the Fe atoms and the large magnetic interface anisotropy $K^{S}_{2,Ni\text{-}Fe}=-93$ μeV/atom of the Ni-Fe interface.

Helpful discussions with J. Lindner and A. Hucht are acknowledged. R.R. thanks the Deutscher Akademischer Austauschdienst for financial assistance. This work was supported by Deutsche Forschungsgemeinschaft and by the U.S. Department of Energy, Contract No. DE-AC3-76SF00098. The financial support by the Access to Research Infrastructure action of the Improving Human Potential Program is acknowledged.

[1] A. Vaterlaus, C. Stamm, U. Meier, M. G. Pini, P. Politi, and D. Pescia, Phys. Rev. Lett. **84**, 2247 (2000), and references therein.
[2] L. Man, W. L. Ling, Silena Y. Paik, H. Poppa, M. S. Altman, and Z. Q. Qiu, Phys. Rev. B **65**, 024409 (2001).
[3] D. P. Pappas, K.-P. Kämper, and H. Hopster, Phys. Rev. Lett. **64**, 3179 (1990).
[4] E. Mentz, A. Bauer, T. Günther, and G. Kaindl, Phys. Rev. B **60**, 7379 (1999).
[5] J. Shen, A. K. Swan, and J. F. Wendelken, Appl. Phys. Lett. **75**, 2987 (1999).
[6] J. P. Pierce, M. A. Torija, J. Shen, and E. W. Plummer, Phys. Rev. B **64**, 224409 (2001).
[7] M. Farle, Rep. Prog. Phys. **61**, 755 (1998).
[8] M. Farle, W. Platow, A. N. Anisimov, P. Poulopoulos, and K.

Baberschke, Phys. Rev. B **56**, 5100 (1997).
[9] R. Vollmer, Th. Gutjahr-Löser, and J. Kirschner, Phys. Rev. B **60**, 6277 (1999).
[10] A. Hucht and K. D. Usadel, J. Magn. Magn. Mater. **198-199**, 493 (1999).
[11] V. Jähnke, J. Güdde, and E. Matthias, J. Magn. Magn. Mater. **237**, 69 (2001).
[12] X. Liu and M. Wuttig, Phys. Rev. B **64**, 104408 (2001).
[13] B. Schirmer and M. Wuttig, Phys. Rev. B **60**, 12 945 (1999).
[14] X. Liu, B. Schirmer, and M. Wuttig, Phys. Rev. B **65**, 224413 (2002).
[15] W. L. O'Brien and B. P. Tonner, Phys. Rev. B **52**, 15 332 (1995).
[16] Dongqi Li, M. Freitag, J. Pearson, Z. Q. Qiu, and S. D. Bader, Phys. Rev. Lett. **72**, 3112 (1994).
[17] C. Won, Y. Z. Wu, H. W. Zhao, A. Scholl, A. Doran, and Z. Q. Qiu, Phys. Rev. B **68**, 052404 (2003).
[18] R. Ramchal, A. Schmid, H. Poppa, M. Farle, Phys. Rev. B **68**, 054418 (2003).
[19] E. Bauer, Rep. Prog. Phys. **57**, 895 (1994).
[20] W. Platow, U. Bovensiepen, P. Poulopoulos, M. Farle, K. Baberschke, L. Hammer, S. Walter, S. Müller, and K. Heinz, Phys. Rev. B **59**, 12 641 (1999).
[21] C. M. Schneider *et al.*, *Magnetism and Structure in Systems of Reduced Dimension*, edited by R. F. C. Farrow *et al.* (Plenum Press, New York, 1993).
[22] M. S. Altman *et al.*, in *Magnetic Materials: Microstructure and Properties*, edited by T. Suzuki, Y. Sugita, B. M. Clemens, K. Ouchi, and D. E. Laughlin, Mater. Res. Soc. Symp. Proc. No. 232 (Materials Research Society, Pittsburgh, 1991), p. 125.
[23] E. Bauer, T. Duden, H. Pinkvos, H. Poppa, and K. Wurm, J. Magn. Magn. Mater. **156**, 1 (1996).
[24] S. Dieluweit, H. Ibach, M. Giesen, and T. L. Einstein, Phys. Rev. B **67**, 121410 (2003).
[25] S. S. Dhesi, H. A. Dürr, and G. van der Laan, Phys. Rev. B **59**, 8408 (1999).
[26] J. Lindner, P. Poulopoulos, R. Nünthel, E. Kosubek, H. Wende, and K. Baberschke, Surf. Sci. **523**, L65 (2002).
[27] W. Platow, M. Farle, and K. Baberschke, Europhys. Lett. **43**, 713 (1998).